

Iodine-Stabilized Cu Nanoparticle Chitosan Composite for Antibacterial Applications

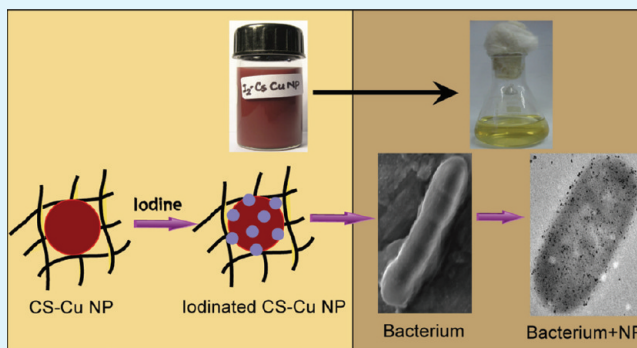
Sadhucharan Mallick,[†] Shilpa Sharma,[‡] Madhuchanda Banerjee,[‡] Siddhartha Sankar Ghosh,^{‡,§} Arun Chattopadhyay,^{*,†,‡} and Anumita Paul^{*,†}

[†]Department of Chemistry, [‡]Centre for Nanotechnology, and [§]Department of Biotechnology, Indian Institute of Technology Guwahati, Guwahati-39, Assam, India

S Supporting Information

ABSTRACT: We report herein the synthesis of a new composite consisting of Cu nanoparticles (NPs) and chitosan (CS), which has been found to be stable in the presence of molecular iodine and has also high antimicrobial activities. The composite could be obtained when aqueous CuSO₄ was treated with hydrazine in the presence of CS. The spherical Cu NPs present in the composite were of average diameters 8±4 nm. The NPs were unstable in atmospheric conditions leading to the formation of oxides of Cu. On the other hand, when molecular iodine was added to the medium following synthesis the NPs were rather stable. Studies of antibacterial property were carried out on Gram-negative green fluorescent expressing *Escherichia coli* bacteria & Gram-positive *Bacillus cereus* bacteria. The minimum inhibitory concentration (MIC) of the iodinated composite on *Escherichia coli* was found to be 130.8 µg/mL, which contained 21.5 µg/mL Cu NPs. This determined value of MIC for Cu NPs was much lower than those reported in the literature. Zeta potential (ζ) measurements supported an attractive interaction between iodinated CS-Cu NP composite and bacteria which was further supported by electron microscopic images. Electron microscopic and flow cytometric studies revealed that the iodinated CS-Cu NP composite was attached to the bacterial cell wall, which caused irreversible damage to the membrane, eventually leading to cell death. Mechanism of bactericidal action of the iodinated composite is discussed in light of our findings.

KEYWORDS: iodine, Cu nanoparticle, chitosan, composite, bactericide, green fluorescent protein



INTRODUCTION

In the past two decades, a substantial body of research work in the syntheses of metal nanoparticles (NPs) has been directed towards creating conditions where optical, chemical, and biological properties of the NPs could be exploited. In this regard, coinage metals (Cu, Ag, and Au) provide special opportunity owing to their biological applications. For example, it has been established that optical and optothermal properties of Au NPs or nanorods could be utilized in healthcare diagnostics and therapeutics such as in hyperthermia treatment of cancer cells.^{1,2} On the other hand, colloidal silver has been used and in recent times Ag NPs have been proposed for antimicrobial and anticancer therapy in the form of either NPs or the NPs present in the composite. However, the use of Ag NPs has been a cause of concern—albeit they are being addressed systematically—especially because of their persistent presence in living systems and lack of any suitable sequestering agent. For example, implications of Ag NPs being present in the environment need to be understood before their widespread use in antibacterial treatments such as in water filter systems and Ag NP lined clothing.³ In this regard, Cu NPs are attractive alternatives because in addition to their catalytic, optical and

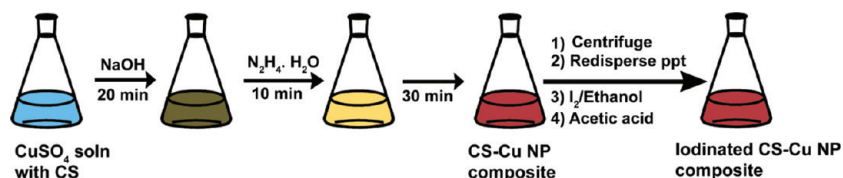
electrically conducting properties they are known to have significant antibacterial and antifungal properties.^{4–15} For example, Esteban-Cubillo and coworkers have demonstrated bactericidal properties of Cu NPs prepared in the matrix of sepiolite.¹⁶ On the other hand, Kelechi C. et al. reported that the antimicrobial activity of acrylated Cu NPs is similar to that of conventional copper based biocides.¹⁰ Additionally, Cioffi, et al.⁹ have reported antifungal and antifouling properties of a Cu NP-polymer composite. M. Taner et al. recently reported synthesis of Ag–Cu nanoalloys and their bactericidal behaviour against *Escherichia coli* (*E. coli*),¹⁷ but Ag known to accumulate in the human body over time, can lead to toxicity such as argyria.¹⁸ Importantly, there are known sequestering agents for Cu^{19,20} in order for their release out of the human body following their use. However, use of Cu NPs still poses a fundamental challenge because of their ease of oxidation especially in an aqueous environment of living systems and in open atmosphere. In this regard, it is also important to address

Received: November 14, 2011

Accepted: February 2, 2012

Published: February 2, 2012

Scheme 1. Schematic Representation of the Procedure Used for the Synthesis of Iodinated CS-Cu NP Composite



the issue of the species involved in antimicrobial or antifungal activities and the mechanism of action. For example, whether the NPs remain as such or get oxidized to Cu^{2+} species is still largely an open question. In addition, the details of the mechanism of action of the NPs still remain to be fully understood. This is where an opportunity lies in terms of developing a reaction condition where Cu NPs would not only be synthesized but also remain stable for sufficiently long time in order for them to be useful.

As a natural response to the demand, several methods have recently been developed for the syntheses of Cu NPs that include thermal reduction,²¹ sono-chemical reduction,²² metal vapor synthesis,²³ chemical reduction,⁷ vacuum vapor deposition,⁸ radiation methods,²⁴ microemulsion techniques,^{25–27} and laser ablation.²⁸ Interestingly, most of these methods utilize oxygen-free environment for the synthesis as the incipient Cu NPs get readily oxidized in the atmosphere.^{7,9,11,22,27,29} For example, Lisiecki et al.²⁷ reported the synthesis of Cu NPs in aqueous solution using sodium dodecyl sulfate as the capping agent where they used the inert environment of a glove box with nitrogen flow to prevent the oxidation of the generated Cu NPs. Further, Joshi et al.²⁹ reported the synthesis of Cu NPs by gamma radiolysis, in an aqueous system under nitrogen atmosphere. Thus there is still a need for the development of a method for the atmospheric synthesis of Cu NPs where the NPs would remain stable for sufficiently long time for their use especially in antimicrobial and antifungal applications.

Herein, we report the development of a new method for the preparation of Cu NPs under atmospheric conditions in the presence of chitosan (CS) as the stabilizing agent and in the form of a composite with CS. Chitosan (CS) is a naturally occurring, cationic polysaccharide composed of (1,4)-linked 2-amino-2-deoxy- β -D-glucose and 2-acetamido-2-deoxy- β -D-glucose units. The polymer has significant content of primary amines and hydroxyl groups thus providing it with a strong affinity towards metal ions, which can be incorporated by simple chelation or by ion exchange, making it an excellent support for synthesis of metal NPs.^{30,31} The synthesis was carried out by reducing Cu^{2+} using hydrazine as the reducing agent and in the presence of CS as the stabilizer. The method produced Cu NPs with average size 8 ± 4 nm. It was further observed that the as-prepared NPs were oxidized rather rapidly (within hours of preparation) in the medium while they were reasonably stable in the presence of hydrazine in the medium or in vacuum dried sample. On the other hand, addition of molecular iodine to the prepared NPs in the medium provided stability to the NPs in the medium which could then be used for antimicrobial studies. In addition, the presence of iodine in the composite also enhanced the antimicrobial activity of Cu NPs. The antimicrobial studies were carried out using green fluorescent protein (GFP) expressing recombinant *E. coli* bacteria.³² Considering that CS itself is antimicrobial, the three-component (Cu NPs, CS and iodine) system provided a new way of antimicrobial action where the minimum inhibitory

concentration (MIC) and minimum bactericidal concentration (MBC) of iodinated CS-Cu NP composite against *E. coli* were found to be 130.8 and 239.4 $\mu\text{g}/\text{mL}$, respectively. Quite a few studies attribute the antimicrobial property of copper and their oxides to the released Cu ions in aqueous medium.^{9,10} On the other hand, our findings from electron microscopic, optical and biochemical studies indicated that iodinated CS-Cu NP composite was attached to the bacterial cell surface, causing irreparable membrane damage followed by membrane disintegration and finally leading to cell death. Importantly, while the Cu NPs contributed to the overall bactericidal activity, atomic absorption spectroscopic measurements indicated that the copper ions, being released - if any, played a minor role in the bactericidal activity of the composite.

EXPERIMENTAL SECTION

Materials and Methods. Copper (II) sulphate pentahydrate ($\text{CuSO}_4 \cdot 5\text{H}_2\text{O}$; Merck, India), chitosan of high molecular weight (75% deacetylated; Sigma-Aldrich Chemical Co.), sodium hydroxide (NaOH, 98%; Merck, India), Hydrazine hydrate solution (80%; Merck, India), acetic acid (glacial, 99–100%; Merck, India) and ethanol were used as received without further purification. Milli-Q grade (resistivity 18.2 $\text{M}\Omega\text{cm}^{-1}$) water was used in all experiments. GFP-expressing recombinant *E. coli* was grown in Luria-Bertani (LB) medium (Himedia, Mumbai, India), *Bacillus cereus* was grown in nutrient broth (NB) (Himedia, Mumbai, India), Iodine and other high purity molecular biology grade chemicals and reagents for agarose gel electrophoresis were obtained from Sigma-Aldrich Chemical Pvt. Ltd., Kolkata, India.

Preparation of Iodinated CS-Cu NP Composite. Chitosan stabilized Cu NPs were synthesized under normal atmospheric conditions, as shown in Scheme 1. For this, 50 mg of chitosan and 40 mg of copper(II) sulphate pentahydrate were added to 50 mL Milli-Q grade water in a 100 mL round bottom flask placed in an oil bath with vigorous stirring and refluxed for 20 min at ~ 100 °C, resulting in a light blue colored solution. To this was added 0.6 mL of 0.6 M NaOH, upon which the color of the solution turned brown. After about 20 min, 0.4 mL of hydrazine hydrate solution was added to the above solution with constant stirring. Within 10 min, a yellow solution was formed. The reaction was allowed to continue for an additional 30 min until a reddish colored solid appeared at the bottom of the round bottom flask. The flask was then taken out from the oil bath and cooled to room temperature.

The solution along with the precipitate was centrifuged at 5300 rpm and pellet washed with milli-Q grade water several times to remove hydrazine. The pellet was then redispersed in 20 mL of 0.25% aqueous acetic acid solution. To that CS-Cu NP redisperse solution was added 300 μL of 0.2 M iodine solution in ethanol, and the solution was mixed thoroughly. The resulting reddish colored solution was characterized and used for antibacterial studies. The supernatant solution was treated with excess $\text{N}_2\text{H}_4\text{NH}_2 \cdot \text{H}_2\text{O}$ to check for any excess of Cu^{2+} present in the medium, which was negative. In other words, all of Cu^{2+} ions present in the medium had reacted. For characterization of the product, the reddish solution was centrifuged, vacuum dried and stored under vacuum before analysis. Further, control experiment in absence of hydrazine hydrate yielded CuO NPs from CuSO_4 , showing that CS did not reduce CuSO_4 to Cu NPs (see the Supporting Information, Figures S1A, S1B, and S1C).

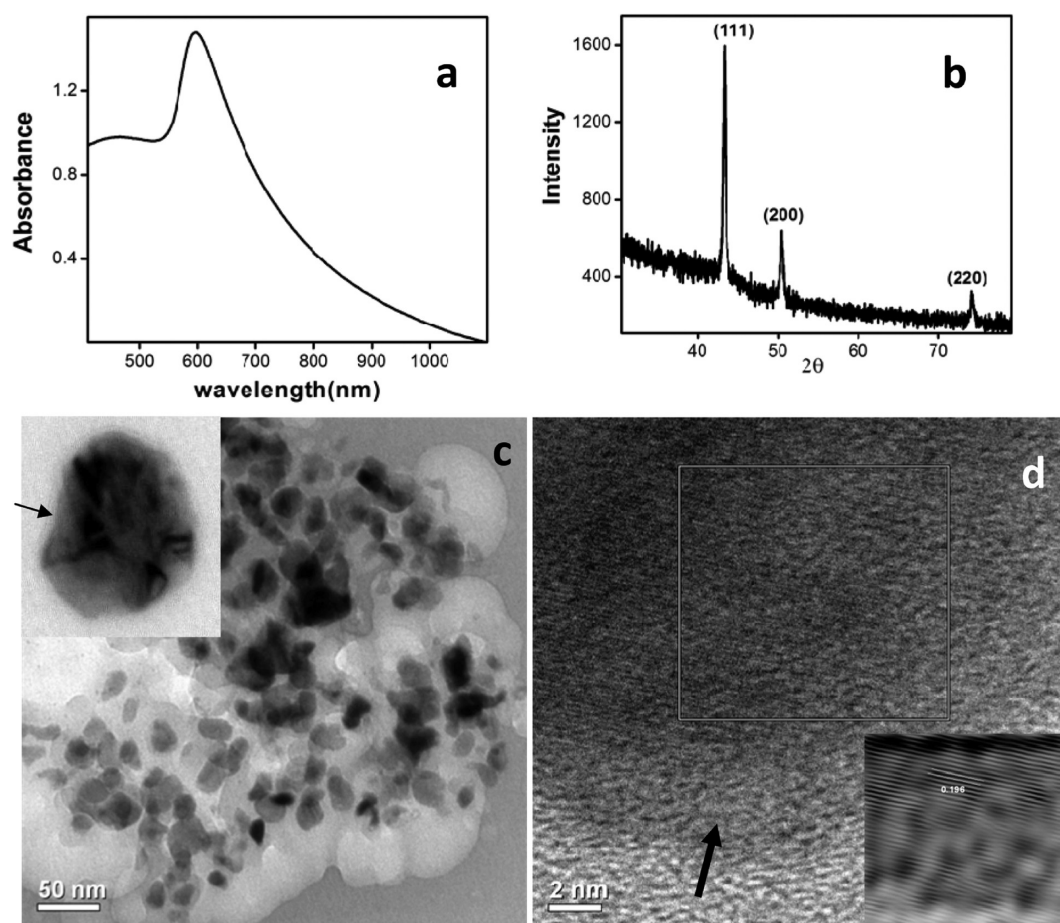


Figure 1. (a) UV–visible spectrum of freshly prepared CS-Cu NP composite. (b) Powder XRD pattern of freshly prepared CS-Cu NP composite. (c) TEM image of freshly prepared CS-Cu NP composite. Inset is TEM image of a single Cu NP. Arrow indicates amorphous layer. (d) High-resolution TEM (HRTEM) image of a particle. Arrow indicates amorphous layer. Inverse Fourier transform of the region indicated in d showing the lattice fringes due to reflection from (111) planes of Cu(0), a better view of which is shown in the inset. The lattice fringe spacing corresponding to (111) plane is 0.196 nm.

Characterization. UV–visible spectra of the reddish dispersion was measured using a Hitachi U 2900 spectrophotometer. Transmission electron microscopy (TEM) was performed using a JEM 2100; Jeol, Peabody, MA) machine operating at a maximum accelerating voltage of 200 keV. 5 μL of sample was drop coated onto a carbon coated copper TEM grid followed by air drying and the resulting grid was then analyzed under TEM. Powder XRD experiments were carried out on a Bruker AXS D8 Advance X-ray diffractometer with Cu K α 1 radiation ($\lambda = 1.54060 \text{ \AA}$), operating at 40 kV and 40 mA. Field-emission scanning electron microscopy (FESEM) measurements were made in a Carl Zeiss, SIGMA VP, instrument. Typically, a 10 μL drop of each sample was deposited on a glass slide, dried, sputter-coated with gold film using a sputter coater (SC7620“Mini”, Polaron Sputter Coater, Quorum Technologies, Newhaven, England), and imaged under the FESEM. Quantitative analysis of the concentration of copper ion release from the composite was performed by using atomic absorption spectrophotometer (model AA240 Varian Inc). For this, the supernatant solution obtained after centrifugation of the composites was investigated by AAS.

Bactericidal Studies. The bactericidal activity was measured by growing GFP-expressing *E. coli* overnight in 150 mL of LB containing ampicillin' medium at pH 6.3. The cells were harvested by centrifugation and re-suspended in 300 μL of LB medium. Three 100 μL portions of the cell suspension were inoculated into 50 mL volumes of fresh LB ampicillin media, without the composite or with composite at different concentrations. The samples were incubated at 37°C. The experiments were performed three times to ensure reproducibility. Gram positive *Bacillus cereus* bacteria were cultured

under the same physiological condition in NB medium. The bacterial growth was monitored by measuring optical density (OD) at 595 nm using a UV–visible spectrophotometer (Lambda; Perkin-Elmer, Fremont, CA, USA) of the sample at different times

Flow Cytometric Assay for Viability Analysis of Bacterial Cells Using GFP-Propidium Iodide Combination. Viability of GFP-expressing recombinant bacterial cells and disruption of membrane integrity was assessed using propidium iodide (PI), which enters only permeable cells, binds DNA, and fluoresces at 620 nm when stimulated by a laser at 488 nm. In viable cells, PI remains in the medium and does not fluoresce; in compromised cells, PI enters the cell through damaged membrane and binds DNA exhibiting fluorescence signals.³³ Briefly, several tubes containing 500 μL (1×10^8 cells/mL) of the recombinant *E. coli* cells and 350 μL of the iodinated composite (at MIC of 130.84 $\mu\text{g}/\text{mL}$ iodinated CS-Cu NP consisting of 127.62 $\mu\text{g}/\text{mL}$ of CS -Cu NP and 3.22 $\mu\text{g}/\text{mL}$ iodine) were incubated at 25°C for various time periods (1 h, 2 h, 4 h and 6 h). After incubation, 1.5 μL of 0.2 mM PI was mixed into each tube and diluted with 150 mM NaCl. Samples were analyzed by a flow cytometer (BD FACS calibur System, BD Biosciences, San Jose, CA). Samples were illuminated with a 15 mW argon ion laser (488 nm), and the fluorescence was detected via $525 \pm 10 \text{ nm}$ (green) and $620 \pm 10 \text{ nm}$ (red) band pass filters. Signals were amplified with the logarithmic mode for side scattering, forward scattering, and fluorescence. In dot plots of fluorescence, different bacterial populations were gated according to the viability stages.

Agarose Gel Electrophoresis of GFP Recombinant Plasmid DNA. Effect of iodinated CS-Cu NP composite on plasmid DNA was

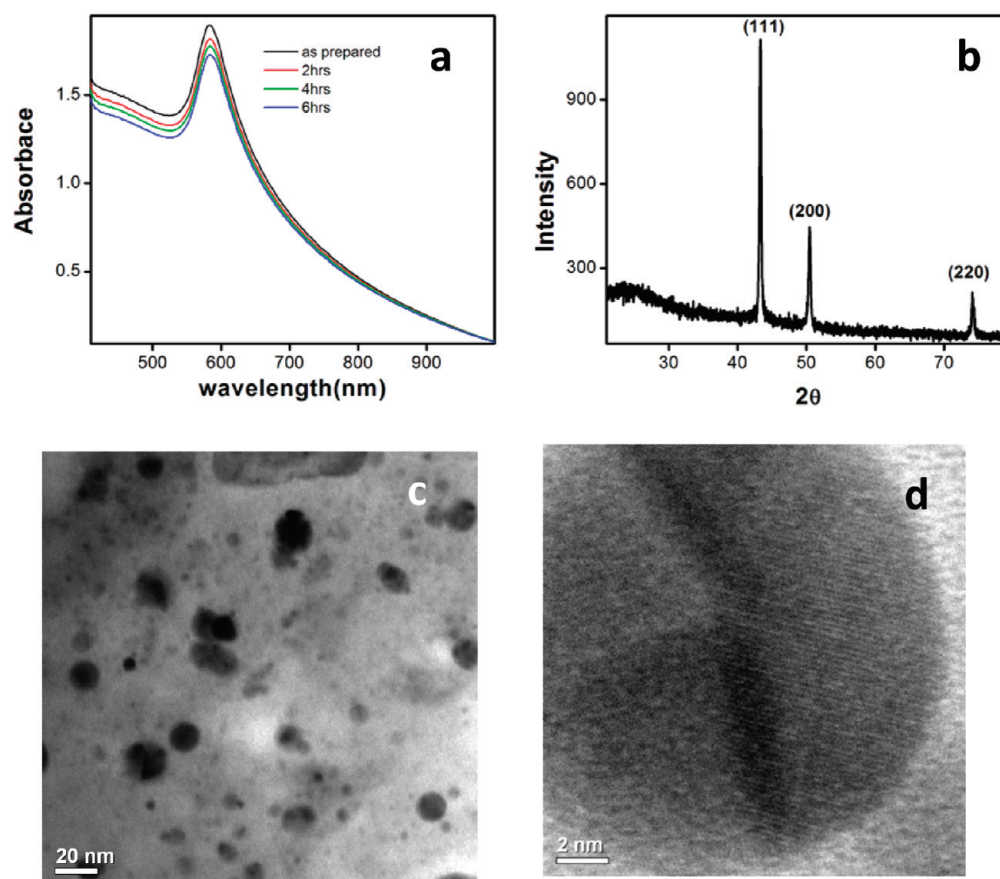


Figure 2. (a) Time-dependent UV–visible spectra of iodinated CS-Cu NP composite as recorded under atmospheric conditions. (b) Powder XRD pattern of freshly prepared iodinated CS-Cu NP composite. (c) TEM image of freshly prepared iodinated CS-Cu NP composite. (d) HRTEM image of a particle showing the lattice fringes corresponding to the (111) planes of copper.

performed by incubating the iodinated CS-Cu NP composite with plasmid DNA at 37 °C. DNA–composite complex formation was checked by 0.8% agarose gel electrophoresis followed by visualization of EtBr stained DNA under UV-transilluminator (see the Supporting Information, Figure S10).

RESULTS AND DISCUSSION

Synthesis and Characterization of the CS-Cu NP Composite: The Role of Chitosan and Iodine. As mentioned earlier the synthesis of Cu NPs in the presence of CS was carried out under normal atmospheric conditions. The reddish solid produced from the reaction of alkaline CuSO_4 and hydrazine (in the presence of CS) was separated from the reaction mixture and then redispersed in water in the presence of acetic acid. UV visible spectrum of this reddish solution showed a prominent peak at 591 nm (Figure 1a), which broadened rapidly in about 2 days (refer to the Supporting Information, Figure S2A). The peak is attributed to the surface Plasmon resonance (SPR) of Cu NPs. The peak disappeared in about 3 days. The peak at 591 is characteristic of formation of Cu NPs in the medium and the dissolution of the solid in acetic acid solution indicated that the NPs were associated with CS (which itself dissolves in acidic condition) and thus a polymer-NP composite might have formed.⁶ It is also important to mention here that the Cu NPs present in the composite were rather unstable as the peak due to NPs was observed to have disappeared within a matter of days. The presence of CS in the composite was confirmed by FTIR studies wherein the peaks

corresponding to CS were present (see the Supporting Information, Figure S4).

Interestingly, powder XRD pattern of the composite recorded after 1 day of synthesis indicated the presence of Cu. The XRD pattern, shown in Figure 1b, indicated the occurrence of diffraction at 2θ values of 43.34, 50.46, and 74.14°, which were indexed as due to diffraction from (111), (200), and (220) planes, respectively, of face-centered-cubic (fcc) crystal planes of Cu(0). The XRD pattern of the composite was matched with the standard powder diffraction data file for copper (face-centered cubic, JCPDS file No. 04–0836). Further, the presence of cupric oxide (CuO) or cuprous oxide (Cu_2O) was not detected in the diffraction. It may be mentioned here that 10 day old samples also showed similar XRD patterns (see Figure S3a in the Supporting Information). This possibly indicates that the surface of Cu NPs present in the composite was possibly oxidized in the atmosphere gradually, which changed the optical extinction spectrum but was not reflected in the XRD pattern. In other words, a thin film (shell) of copper oxide grown from the Cu NP might have affected the optical properties of the Cu NPs inside, but the metal was still present there. It has been established that modification of the surface of metal NPs by deposition of another metal or even polymer may lead to disappearance of the characteristic SPR of the original metal

That the Cu NPs were synthesized and present in the composite was further confirmed by TEM measurements. As shown in Figure 1c, particulates were formed in the medium

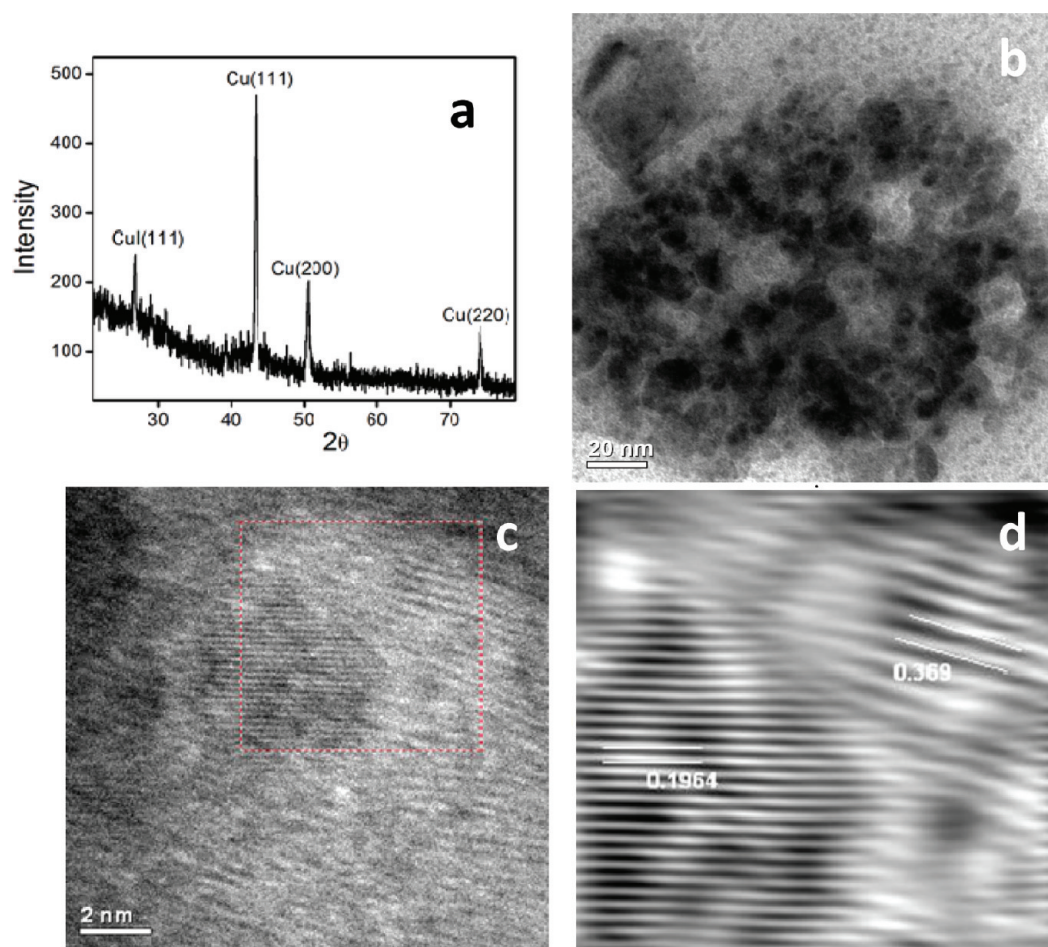


Figure 3. (a) Powder XRD pattern of 10 day old iodinated CS-Cu NP composite. $2\theta = 26.84^\circ$ is the diffraction angle of CuI (111) plane. (b) TEM image of iodinated CS-Cu NP composite of 10 day old sample. (c) HRTEM of the 10 day old iodinated CS-Cu NP composite showing the presence of lattice fringes corresponding to the (111) planes of copper and CuI. (d) Inverse Fourier transform of selected region in c showing the lattice fringes corresponding to the (111) planes of copper and copper iodide. The lattice fringe spacing corresponding to (111) plane of copper and copper iodide are 0.196 and 0.369 nm, respectively.

with average particle size of 17 ± 4 nm. HRTEM image of a particle, shown in Figure 1d clearly indicated crystalline nature of the same. Additionally, the lattice space of 0.196 nm measured from the image (Figure 1d, inset) indicated the presence of crystalline Cu. This matched well with the reported literature value for the lattice fringe of (111) planes of copper.^{11,34} A careful examination of the edges of Cu NP (Figure 1d) shows that the lattice fringes do not extend to the periphery, but rather give way to a thin region of amorphous growth, probably due to oxide formation. TEM image in Figure 1d also shows such an amorphous layer covering the surface of Cu NP. Further, TEM image of 10 day old samples (see the Supporting Information, Figure S3b) show extensive agglomeration of the Cu NPs into larger particles of ~ 50 – 200 nm in sizes. The broadening of the SPR band in aged samples is probably due to a combination of oxidation and agglomeration of the Cu NPs in the composite. This fact is consistent with the XRD results of the aged sample, which still show the presence of peaks due to copper. Thus the present method provided a composite of Cu NP and CS, where the Cu NP surface might have been oxidized slightly in atmosphere, which was sufficiently thin not to alter the NP but might have contributed to the loss of extinction spectrum.

It is understandable that the utility of the NPs in the composite gets reduced when the NPs themselves are prone to oxidation and agglomeration under atmospheric condition. This is especially true when application such as in antimicrobial activity, which is an important aim of the present study, is involved. This problem was alleviated by using molecular iodine in order to stabilize the NPs over a longer period of time. When the composite was redispersed into dilute acetic acid solution followed by treatment with molecular iodine, the color of the composite still retained its original reddish nature. The UV-visible spectrum consisted of a sharp peak at 583 nm (Figure 2a). The shift in the peak may be due to the presence of iodine on the surface of the NPs thereby changing the dielectric constant of the medium in the immediate vicinity of the NPs, i.e., surrounding the NPs. Interestingly, in the presence of the iodine, the peak corresponding to Cu NPs was rather stable.³⁵ As is clear from Figure 2a, for the first 6 h the change in the peak intensity was minimal, although there was a systematic decrease in the background scattering thereby reducing the overall intensity. Further, the peak due to Cu NPs was clearly present for the first 3 days, although the background scattering was continuously decreasing (refer to the Supporting Information, Figure S2b). In addition, the broadening of the peak with time was also slower in the presence of iodine than in

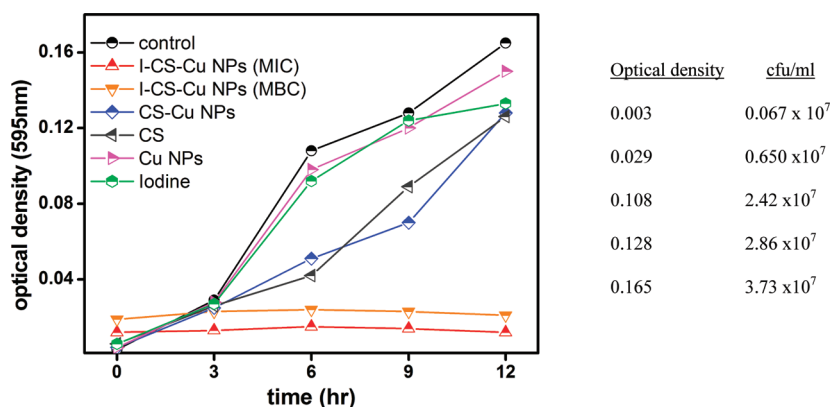


Figure 4. Growth curve of GFP recombinant *E. coli* in the presence of the following (as also indicated in the legends). Control, 0.02 M acetic acid and 6 μL of ethanol only in LB media; I-CS-Cu NPs (MIC), iodinated CS-Cu NP composite at 130.84 $\mu\text{g}/\text{mL}$; I-CS-Cu NPs (MBC), iodinated CS-Cu NP composite at 239.4 $\mu\text{g}/\text{mL}$; CS-Cu NPs, CS-Cu NPs composite at 127.62 $\mu\text{g}/\text{mL}$; CS, chitosan at 106.07 $\mu\text{g}/\text{mL}$; iodine, iodine at 3.22 $\mu\text{g}/\text{mL}$; and Cu NPs, Cu NPs at 21.55 $\mu\text{g}/\text{mL}$.

its absence. Essentially, UV–visible spectroscopic studies indicated that the Cu NPs in the composite were relatively more stable in presence of iodine than in its absence. The stability could be provided by the formation of trace amounts of I atoms on the Cu NP surface. Molecular iodine is known to dissociate to iodine atoms on clean copper surfaces.^{36,37} On the other hand, under normal atmospheric conditions and in absence of iodine, the NPs become unstable possibly because of surface oxidation and agglomeration. Powder XRD patterns of the iodinated CS-Cu NP composite, when the sample was prepared within 1 h of addition of iodine, indicated that they were rather stable (Figure 2b). This was evidenced by the presence of all three peaks corresponding to (111), (200), and (220) occurring at 2θ values 43.34, 50.46, and 74.14° respectively. Further, TEM images of the sample corroborated the stability of the NPs in the presence of iodine as there was hardly, if any, agglomeration and oxidation (Figure 2c). Also the Cu NPs were spherical, much smaller in size in presence of iodine (figure 2c) with measured average size of 8 ± 4 nm. In the HRTEM image in Figure 2d lattice spacing matched with that of Cu metal and the fringes were found to extend all the way to the edge of the NP, indicating the absence of amorphous oxide formation on the surface of the NP. Thus the composite in the presence of iodine would be a good candidate for antimicrobial studies because of its enhanced stability. It is also important to mention here that the stability of Cu NPs in the presence of iodide has been reported recently.³⁵

That the stability of Cu NPs in the composite was enhanced in the presence of molecular iodine is clear from the results of the experiments mentioned above. However, we were further interested in finding the mechanism of stability and thus probed the NPs in the composite treated with iodine. This was pursued by recording the powder XRD and TEM of the composite treated with molecular iodine for 10 days. Figure 3a shows the powder XRD patterns of the sample. As is clear from the figure, the pattern consisted of peaks due to Cu (111), (200), and (220) occurring at 2θ values 43.34, 50.46, and 74.14°, respectively. On the other hand, there was an additional peak occurring at 26.73° that is ascribed to the presence of CuI and the diffraction is due to (111) plane of the salt. This means that the composite even after 10 days retained Cu NPs, although formation of CuI took place in the presence of iodine. Further, TEM measurements indicated that (Figure 3b) that

although there were some degree of agglomeration with time, the particle largely retained their size and thus were stable. On the other hand, HRTEM image of a particle indicated the presence of Cu and CuI as the lattice spacing of 0.196 nm and 0.369 nm were both observed in the same image. That the lattice of CuI was present indicated conversion of nanocrystals of Cu into CuI nanocrystals, possibly in the form of a core-shell structures.

To sum up, we find that both CS and iodine have different roles in stabilization of Cu NPs. CS is a naturally occurring, cationic polysaccharide composed of (1,4)-linked 2-amino-2-deoxy- β -D-glucose and 2-acetamido-2-deoxy- β -D-glucose units, and is able to physisorb on Cu surface because of its significant content of primary amines and hydroxyl groups. In our CS-Cu NP composite, we observed that CS stabilized the Cu NPs and slowed down their aerial oxidation. However CS was unable to prevent the agglomeration of the Cu NPs and after 4 h the sample started showing agglomeration of Cu NPs (i.e., Figure S2A in the Supporting Information). The interaction of molecular iodide on copper surfaces has been studied extensively and reported in the literature. On copper surfaces, molecular iodine dissociatively chemisorbs to form CuI films.³⁸ In our I-CS-Cu NP composite, where we used molecular iodine, we also observed the formation of CuI on the surface of Cu NPs, which inhibited its agglomeration (Figure 3b). This is consistent with the fact that in the iodine-CS-Cu NP composite the ratio of Cu:I₂ used during synthesis was 26.7:1, i.e., there was excess of Cu in comparison with I. Thus in our I-CS-Cu NP sample, in which both CS and molecular iodine were present, Cu NPs are stable towards oxidation and agglomeration for about 4 days in ambient conditions.

Antibacterial Studies of the Iodinated CS-Cu NP Composite. Determination of MIC and MBC on GFP Expressing *E. coli*. The bactericidal activity of the iodinated CS-Cu NP composite was determined on GFP-expressing *Escherichia coli* (*E. coli*) bacteria. Turbidity tests indicated that freshly prepared iodinated CS-Cu NP composite exhibited superior bactericidal activity as opposed to aged samples. Hence for antibacterial studies only freshly prepared samples (within 6 h of preparation) of iodinated CS-Cu NPs were used. From the results reported above, it is clear that such samples used underwent minimum changes thus ensuring reproducibility of the results with maximum effectiveness of the composite. In order to determine the MIC and MBC, 1 \times

10^8 cfu/mL of GFP-expressing *E. coli* were inoculated into Luria-Bertani (LB) medium supplemented with various concentrations of the composite (i.e. in the presence of iodine) and grown overnight at 37°C. The minimum concentration of the iodinated CS-Cu NP composite at which microbial growth was measurably inhibited was taken to be the MIC. Thus MIC was the concentration of the iodinated composite where no visual turbidity of the culture was observed. The cultures that were not turbid were reinoculated into fresh LB containing ampicillin at 100 µg/mL. The MBC of the iodinated Cs–Cu NP composite was considered to be the minimum concentration of the composite that prevented growth of the bacterial cells following reinoculation, as observed visually by the lack of turbidity. Control experiments were performed with acetic acid and ethanol only. For comparison, the antibacterial activities of the CS-Cu NP composite, chitosan, and iodine towards the recombinant GFP-expressing *E. coli* were also measured.

The results of the antimicrobial activity of the iodinated composite are shown in Figure 4. The MIC of the iodinated composite was found to be 130.84 µg/mL, which consisted of 127.62 µg/mL of CS-Cu NP composite and 3.22 µg/mL iodine. The corresponding MBC (239.4 µg/mL) contained 233.50 µg/mL CS-Cu NP and 5.9 µg/mL iodine. In the above concentrations of the iodinated CS-Cu NPs composites, the quantity of Cu NP was 21.55 µg/mL for MIC and 39.43 µg/mL for MBC, respectively. These determined values of MIC for Cu NPs are much lower than those reported for Cu NPs in the literature^{13–15} Control samples with 0.02 M acetic acid and 6 µL of ethanol only in LB media showed no growth inhibition (Figure 4). The doses at which Cu NPs can independently show antibacterial activity (MIC) has been reported to be 60–150 µg/mL.^{13–15} In our case, separate experiments showed that freshly prepared Cu NPs (without CS and iodine) above 468.2 µg/mL inhibited growth of the bacteria in LB medium. Clearly, iodinated CS-Cu NP composite exhibited higher antibacterial activity at much lower dose of Cu NPs in comparison to the bactericidal dose of the individual components, i.e. MIC of chitosan is known to be 468 µg/mL towards *E. coli*^{39,40} and MIC of iodine towards *E. coli* is 155.6 µg/mL^{41,42} and, of course, that of Cu as mentioned before. This is also corroborated by our results shown in Figure 4, where we observe that individual components at their individual concentrations (in the composite) either did not exhibit antibacterial properties (i.e., 21.55 µg/mL Cu NP and 3.22 µg/mL iodine) or exhibited limited bactericidal properties (i.e., 106.07 µg/mL CS) when present as CS-Cu NP composite. However, when present as iodinated composite as in I-CS-Cu NPs (MIC), they inhibited the growth of *E. coli*. Furthermore, growth of GFP expressing *E. coli* was monitored up to 24 h under various treated conditions with no apparent changes in profile (see Figure S5 in the Supporting Information). The MIC value of our turbidity experiments was also substantiated by plate counts of GFP expressing recombinant *Escherichia coli* treated with I-CS-Cu NPs composites (239.4 µg/mL at MBC dose) in a dilution experiment (see Table S1 in the Supporting Information).

In addition, the MIC of I-CS-Cu NP composite on Gram positive *Bacillus cereus* was found to be 165.13 µg/mL, which contained 27.19 µg/mL Cu NPs. The corresponding MBC of I-CS-Cu NP composite was 275.86 µg/mL, which contained 45.42 µg/mL Cu NPs. The values were slightly higher than Gram negative *E. coli* bacteria.

Fluorescence microscopic investigation (see the Supporting Information, Figure S7) with the GFP-expressing *E. coli* bacteria indicated that at the MIC of the iodinated composite, the bacterial population did not grow appreciably after 3 h. On the other hand, at MBC, that bacterial population was obliterated and hardly any bacterium could be observed to be present 3 h after treatment. However, in the control sample, the bacteria grew within the time period of measurement.

Cytometric Measurement of Cell Membrane Damage.

The effect of the composite on the bacteria especially the development of porosity on their cell was further investigated using cytometry. In general, flow cytometric assessment of bacterial cell viability in response to a bactericidal agent typically reveals the existence of four different cell populations corresponding to living, compromised, dead and lysed. Also, it is known that bacterial permeability to nucleic acid staining dye such as propidium iodide (PI) is associated with the occurrence of substantial damage to the membrane, indicating alteration of cell membrane potential, which finally causes cell death. Thus when the cell is not affected by the agent, then green fluorescence (from GFP of the recombinant bacteria) is observed, as PI does not fluoresce as it remains in the medium. On the other hand, when the cells are compromised and membrane porosity is developed, PI could enter the cell and bind to DNA, showing red fluorescence in addition to green fluorescence. However, when the cells are dead cells, the GFP leaks out and thus only red fluorescence is observed. Finally, lysed cells are devoid of fluorescence. Thus measurements of fluorescence could reveal the population of different cells (as above) leading one to better understanding of the working of the antimicrobial agent.

In the present study, bacterial cells, when treated with MIC of iodinated CS-Cu NP composite and incubated for different time periods, say 1, 2, 4, and 6 h, showed a gradual shift of population from viable to compromised cells (Figure 5). Results showed negligible amount of dead or lysed cells in the above time periods. Interestingly, after 1 h of treatment almost all the cells were found to be living and healthy. However, with the progression of time, the population of compromised cells gradually increased and reached its maximum at 6 h, where almost 50% of the total cell population appeared to have been compromised. Incidentally, parallel to this, the untreated group of bacteria (control) exhibited a smaller number of compromised cells. The results are further detailed in Table 1. The results suggested that the iodinated CS-Cu NP composite caused irreparable damage to the bacterial cell membrane, which began as early as 2 h following treatment.

Interaction of the composite with bacterial cells was further studied by TEM and FESEM. FESEM images of both the untreated and the composite treated GFP recombinant *E. coli* are shown in images a and b in Figure 6. The sample for composite treated bacteria was kept in the medium (with the concentration of the composite being at MIC, i.e., 130.84 µg/mL) for 3 h prior to evaporation for sample preparation. It is interesting to observe from images a and b in Figure 6 that although untreated bacterium was healthy and of usual surface morphology, the one being treated with the composite clearly was different and the cell was covered with particles. The diameter of the particles (~5–15 nm) indicated that the particles were made of Cu NPs as they were the same as in the composite (the particle sizes as measured from TEM, Figure 2c). TEM investigations of the composite treated bacteria further supported the attachment of the composite to the cells.

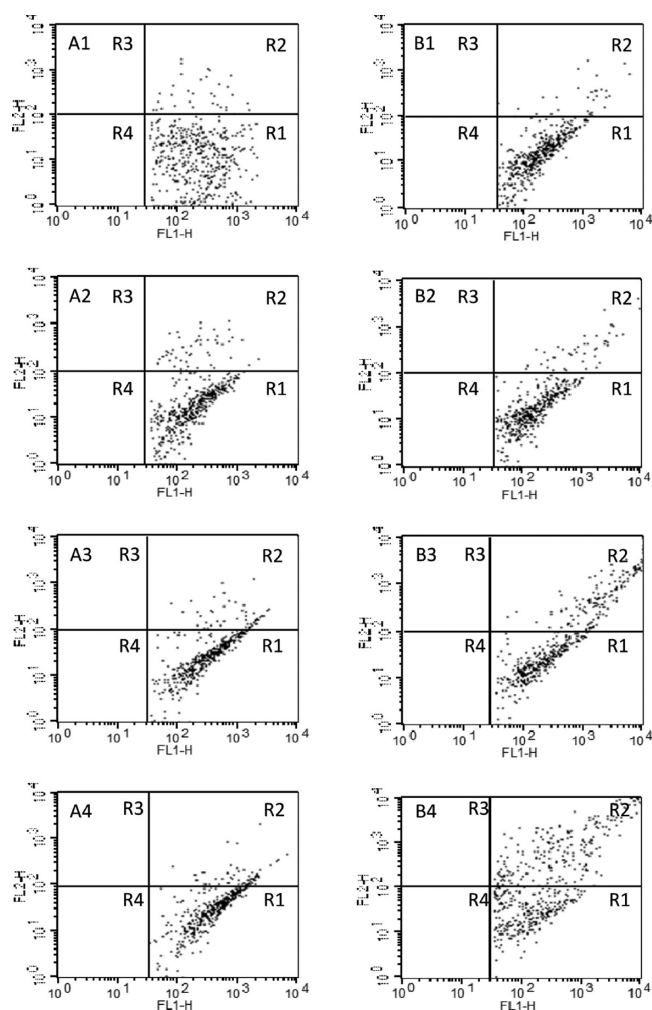


Figure 5. Dot plots showing populations of *E. coli* cells (GFP expressing stained with PI) at different viability stages, measured by flow cytometry at different time points treated with iodinated CS-Cu NP composite. Series A refers to untreated cells and series B refers to cells treated with MIC (130.84 $\mu\text{g}/\text{mL}$) of the composite. Different viability stages are denoted as R1 (live), R2 (compromised), R3 (dead), and R4 (lysed) cells.

For example, as shown in Figure 6c, darker spots of particle were observed to have been superimposed on the image of a bacterium. This is also evidenced from TEM image (see Figure S8a in the Supporting Information) and SAED (see Figure S8b in the Supporting Information), which further confirmed that the NPs attached to the cell wall were Cu. Thus the composite was indeed interacting with the bacterium. Also, the image of a bacterium being damaged possibly because of development of porosity on its cell wall (Figure 6d) further supports the interaction leading to cell death via cell wall damage. It is

important to mention here that the NPs (in the composite) being present on the cell surface retained their individual character as the particle sizes when attached to the bacterium and as-prepared were comparable. In other words, no agglomeration of NP was observable when the composite was attached to the bacterial cell surface. Further, it is important to note here that XRD pattern of the composite-treated bacteria, where the sample was prepared 4 h after treatment, indicated that Cu NPs were still present in the medium as the diffraction pattern due to (111), (200), and (220) planes could still be observed, although peaks due to CuI were also present (see the Supporting Information, Figure S9). It may also be noted that aged samples of the composite, when formation of CuI was observed extensively, did not show antibacterial activity at a concentration of 130.84 $\mu\text{g}/\text{mL}$ (MIC) as was probed using turbidity test.

Polycationic chitosan is well known to interact with negatively charged cell envelop which permeabilizes the cell membrane leading to leakage of intracellular components.^{43–46} Zeta potential (ζ) measurements were performed to determine the charge of iodinated CS-Cu NP composite, chitosan, iodine in aqueous solution at pH 6.3. Zeta potential (ζ) values were measured using Delsa Nano submicrometer particle size and zeta potential particle analyzer (PN A54412AA, Beckman Coulter). Zeta potential values at pH 6.3 were as follows: iodine, -75.37 mV; chitosan, $+59.57$ mV; and iodinated CS-Cu NP composite, $+36.49$ mV. Further, zeta potential measurements on various strains of *E. coli* in pH ranges 2 to 9 have shown that the surface charge of bacterial cells is negative.^{47,48} Hence, presumably, *E. coli* cells negative surface charge adheres to the positively charged iodinated CS-Cu NP composite through electrostatic interactions. Once the composite gets attached to the bacterial cell wall, Cu NPs possibly get attached to sulfur-containing proteins⁴⁹ of bacterial cell membrane, leading to greater permeability of the membrane, causing leakage of proteins and other intracellular constituents and death of bacteria.

Gel retardation assay indicated the possibility of attachment of iodinated CS-Cu NP composite with plasmid DNA (see the Supporting Information, Figure S10). We observed that plasmid DNA treated with the composite did not enter the lane during gel electrophoresis. This could be due to attachment of DNA with the composite, which finally led to increase in molecular size. Thus, it is probable that DNA of the compromised bacterial cell might well have been attached to the composite after perforation of the cell wall by Cu NPs present in the composite, ultimately killing it. This observation is similar to our previous study.³³

It is important to understand the antimicrobial activity of the composite vis-à-vis the presence of Cu NPs. In this regard, several studies attribute the antibacterial property of copper to the Cu^{2+} ions released in aqueous medium.^{9,10} We have

Table 1. Percentage of Total *E. coli* Cells Untreated and Treated with Iodinated CS-Cu NP Composite (130.84 $\mu\text{g}/\text{mL}$) at Different Viability Stages during Different Time Points Measured by Flow Cytometry. Percentages of Dead and Lysed Cells Were Negligible

	untreated (% of total cells)				treated (% of total cells)				
	time (h)								
	1	2	4	6	1	2	4	6	
live	91.95	90.26	86.24	85.50	92.31	87.88	66.89	51.09	
compromised	8.05	9.73	13.74	14.39	7.12	12.11	33.11	48.91	

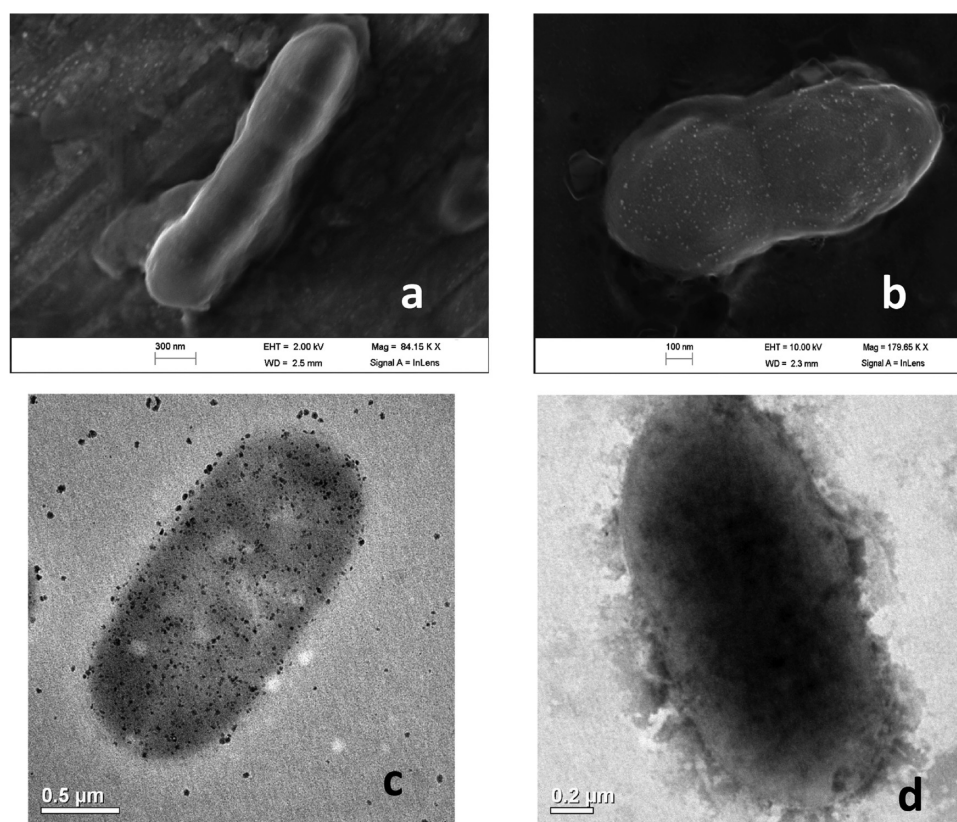


Figure 6. (a) Field-emission scanning electron micrograph of GFP expressing recombinant *E. coli* cells and (b) *E. coli* cells treated with 130.84 μg/mL (MIC) iodinated CS-Cu NP composite in liquid LB medium for 3 h. (c) TEM image of a GFP expressing recombinant *E. coli* cell treated with 130.84 μg/mL (MIC) iodinated CS-Cu NP composite in liquid LB medium for 3h. (d) TEM of a cell treated with MIC of iodinated CS-Cu NP composite showing damage.

investigated whether in our composite too, the antibacterial properties of Cu NP is due to released Cu^{2+} ions, using atomic absorption spectroscopic (AAS) studies. AAS data in the Supporting Information, Figure S6A, show that the freshly prepared iodinated CS-Cu NP composite at MIC (130.84 μg/mL composite containing 21.55 μg/mL Cu NPs) slowly released Cu^{2+} ions into the aqueous medium such that at ~1.5 h the concentration of Cu^{2+} in solution was 17.8 ppm, which increased up to 32.2 ppm in ~4 h. Note that this time was greater than the time taken to inhibit the growth at MIC, which is 3 h as is clear from Figure 4. Moreover, 5 day old samples where the concentration of Cu^{2+} ions was 46 ppm did not show antibacterial property at MIC of the composite.

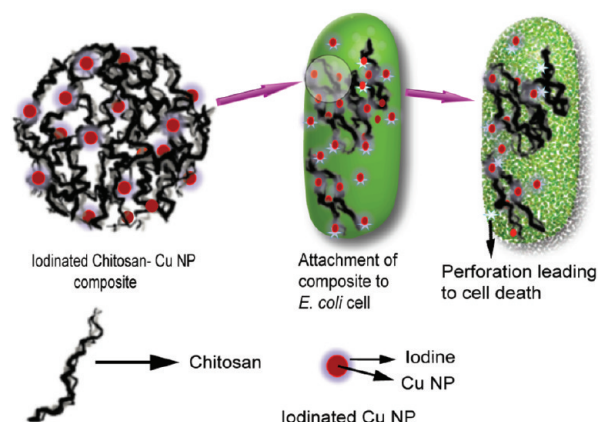
To directly probe the contribution of Cu ions to the bactericidal activity of the composite, we carried out growth analysis studies in presence of different strengths of CuSO_4 solutions and that of a control experiment without Cu ions (see the Supporting information, Figure S6B). In these solutions, the concentrations of Cu ion was similar to those which leached from the iodinated CS-Cu NP composite between ~1.5 h to 5 days. It was found that there was no retardation of bacterial growth due to Cu ions. This indicated that Cu ions that release from the iodinated CS-Cu NP have little or no effect on the bactericidal potency of the composite.

We thus conclude that released Cu^{2+} ions did not play an important role in killing the bacteria in our studies. Rather it's the attachment to the cell wall of the Cu NPs from the iodinated CS-Cu NP composite which perforated the cell wall causing leakage of proteins and other intracellular constituents and ultimately caused cell death.

Essentially, various studies indicated that the bacterial cells were attached to the composite, possibly because of their opposite charges. Thus, while the polymer helped keep the bacterium attached, the Cu NPs present in there possibly led to perforation of the cell wall causing irreparable damage to the membrane. The iodine present on the surface of the NP not only stabilized them but also may have contributed to the overall activity as it is a known antimicrobial agent. The three components working in coordination led the bacteria to become unviable and finally causing cell death. A schematic representation of the process is shown in Scheme 2.

Finally, a question may arise about the feasibility of the use of the present composite in real antimicrobial applications. First of all, the CS-Cu NP composite could be isolated as solid powder following synthesis and weighed amount could then be stored in evacuated ampules. This would add not only to long term stability but also to ease in transportability. Similarly, molecular iodine could be made available in another container. A dispersion of the composite and iodine in solution could then be prepared on site for appropriate use. This concoction could then be used for external and internal applications. Further, one could conceive of making a paste out of the components for wound dressing. In addition, our observations of enhanced stability of the dried powder form of iodinated CS-Cu NP composite (used herein for XRD measurement) indicated its possible use in the form of powder.

Scheme 2. Schematic Representation of the Proposed Mechanism of Antibacterial Action of the Iodinated CS-Cu NP Composite



CONCLUSION

We have reported herein the synthesis of a new CS-Cu NP composite. The composite as such in the atmosphere was not stable and was prone to oxidation. However, in the presence of molecular iodine the composite was rather stable. The added stability of the iodinated composite permitted its efficacy as a potent antimicrobial agent. Studies on GFP expressing *E. coli* bacteria revealed the effectiveness of the composite. Polycationic chitosan interacted with the negatively charged cell envelope. In addition, Cu NPs possibly got attached to sulfur-containing proteins of bacterial cell membrane. This caused permeability of the membrane leading to leakage of proteins and other intracellular constituents and death of bacteria.

Interestingly, the MIC and MBC of Cu NPs (when present in the iodinated composite) against *E. coli* bacteria were found to be 21.5 and 39.4 $\mu\text{g}/\text{mL}$, respectively, which are much lower than the values reported for Cu NPs only. AAS studies and growth analysis in presence of Cu ions also indicated the role of Cu NPs rather than leached out Cu^{2+} ions for the killing activity against bacteria. That there are known sequestering agents for Cu from human body adds value to a new composite which might be much less of health and environmental hazards compared to Ag NP-based materials. That the iodinated composite has been found to have antagonistic activity against both Gram positive and Gram negative bacteria augurs well for its possible use as a general antimicrobial agent.

ASSOCIATED CONTENT

Supporting Information

Additional results based on spectroscopic studies, microscopic studies, agarose gel electrophoresis, and dilution experiments by plate count method are available. This material is available free of charge via the Internet at <http://pubs.acs.org/>.

AUTHOR INFORMATION

Corresponding Author

*E-mail: arun@iitg.ernet.in (A.C.); anumita@iitg.ernet.in (A.P.).

Notes

The authors declare no competing financial interest.

ACKNOWLEDGMENTS

We thank Department of Science and Technology (DST), Department of Biotechnology (DBT), and Council of Scientific and Industrial Research (CSIR) for funds. S.M. thanks CSIR for a fellowship (09/731(0061)/2008-EMR-I). Assistance from Central instruments facility (CIF) IIT Guwahati is gratefully acknowledged.

REFERENCES

- Huang, X. H.; Jain, P. K.; El-Sayed, I. H.; El-Sayed, M. A. *Nanomedicine* **2007**, *2*, 681–693.
- Jain, P. K.; Huang, X. H.; El-Sayed, I. H.; El-Sayed, M. A. *Acc. Chem. Res.* **2008**, *41*, 1578–1586.
- Jain, P.; Pradeep, T. *Biotechnology and Bioeng.* **2005**, *90*, 59–63.
- Vukojevic, S.; Trapp, O.; Grunwaldt, J.-D.; Kiener, C.; Schuth, F. *Angew. Chem., Int. Ed.* **2005**, *44*, 7978–7981.
- Ressler, T. B.; Kniep, L.; Kasatkin, I.; Schlogl, R. *Angew. Chem., Int. Ed.* **2005**, *44*, 4704–4707.
- Creighton, J. A.; Eadon, D. G. *J. Chem. Soc., Faraday Trans.* **1991**, *87*, 3881–3891.
- Huang, H. H.; Yan, F. Q.; Kek, Y. M.; Chew, C. H.; Xu, G. Q.; Ji, W.; Oh, P. S.; Tang, S. H. *Langmuir* **1997**, *13*, 172–175.
- Liu, Z.; Bando, Y. *Adv. Mater.* **2003**, *15*, 303–305.
- Cioffi, N.; Torsi, L.; Ditaranto, N.; Tantillo, G.; Ghibelli, L.; Sabbatini, L.; Bleve-Zacheo, T.; D'Alessio, M.; Zambonin, P. G.; Traversa, E. *Chem. Mater.* **2005**, *17*, 5255–5262.
- Anyagou, K. C.; Fedorov, A. V.; Neckers, D. C. *Langmuir* **2008**, *24*, 4340–4346.
- Wei, Y.; Chen, S.; Kowalczyk, B.; Huda, S.; Gray, T. P.; Grzybowski, B. A. *J. Phys. Chem. C* **2010**, *114*, 15612–15616.
- Kim, Y. H.; Lee, D. K.; Cha, H. G.; Kim, C. W.; Kang, Y. C.; Kang, Y. S. *J. Phys. Chem. B* **2006**, *110*, 24923–24928.
- Yoon, K. -Y.; Byeon, J. H.; Park, J. -H.; Hwang, J. *Sci. Total Environ.* **2007**, *373*, 572–575.
- Ruparelia, J. P.; Chatterjee, A. K.; Duttgupta, S. P.; Mukherji, S. *Acta Biomater.* **2008**, *4*, 707–716.
- Raffi, M.; Mehrwan, S.; Bhatti, T. M.; Akhter, J. I.; Hameed, A.; Yawar, W.; Hasan, M. M. *ul. Ann. Microbiol.* **2010**, *60*, 75–80.
- Esteban-Cubillo, A.; Pecharroman, C.; Aguilar, E.; Santaren, J.; Moya, J. S. *J. Mater. Sci.* **2006**, *41*, 5208–5212.
- Taner, M.; Sayar, N.; Yulug, I. G.; Suzer, S. *J. Mater. Chem.* **2011**, *21*, 13150–13154.
- Fung, M. C.; Bowen, D. L. *Clin. Toxicol.* **1996**, *34*, 119–126.
- Gaggelli, E.; Kozlowski, H.; Valensin, D.; Valensin, G. *Chem. Rev.* **2006**, *106*, 1995–2044.
- Cater, M. A.; Fontaine, S. L.; Shield, K.; Deal, Y.; Mercer, J. F. B. *Gastroenterology* **2006**, *130*, 493–506.
- Dhas, N. A.; Raj, C. P.; Gedanken, A. *Chem. Mater.* **1998**, *10*, 1446–1452.
- Kumar, R.V.; Mastai, Y.; Diamant, Y.; Gedanken, A. *J. Mater. Chem.* **2001**, *11*, 1209–1213.
- Vitulli, G.; Bernini, M.; Bertozzi, S.; Pitzalis, E.; Salvadori, P.; Coluccia, S.; Martra, G. *Chem. Mater.* **2002**, *14*, 1183–1186.
- Casella, I. G.; Cataldi, T. R. I.; Guerrieri, A.; Desimoni, E. *Anal. Chim. Acta* **1996**, *335*, 217–225.
- Lisiecki, I.; Pileni, M. P. *J. Am. Chem. Soc.* **1993**, *115*, 3887–3896.
- Qi, L.; Ma, J.; Shen, J. *J. Colloid Interface Sci.* **1997**, *186*, 498–500.
- Lisiecki, I.; Billoudet, F.; Pileni, M. P. *J. Phys. Chem.* **1996**, *100*, 4160–4166.
- Yeh, M. S.; Yang, Y. S.; Lee, Y. P.; Lee, H. F.; Yeh, Y. H.; Yeh, C. S. *J. Phys. Chem. B* **1999**, *103*, 6851–6857.
- Joshi, S. S.; Patil, S. F.; Iyer, V.; Mahumuni, S. *Nanostruct. Mater.* **1998**, *10*, 1135–1144.
- Hardy, J. J. E.; Hubert, S.; Macquarrie, D. J.; Wilson, A. *J. Green Chem.* **2004**, *6*, 53–56.

- (31) Murugadoss, A.; Chattopadhyay, A. *Nanotechnology* **2008**, *19*, 015603 (9pp).
- (32) Gogoi, S. K.; Gopinath, P.; Paul, A.; Ramesh, A.; Ghosh, S. S.; Chattopadhyay, A. *Langmuir* **2006**, *22*, 9322–9328.
- (33) Banerjee, M.; Mallick, S.; Paul, A.; Chattopadhyay, A.; Ghosh, S. S. *Langmuir* **2010**, *26*, 5901–5908.
- (34) Hansen, P. L.; Wagner, J. B.; Helveg, S.; Rostrup-Nielsen, J. R.; Clausen, B. S.; Topsoe, H. *Science* **2002**, *295*, 2053–2058.
- (35) Kapoor, S.; Joshi, R.; Mukherjee, T. *Chem. Phys. Lett.* **2002**, *354*, 443–448.
- (36) Lin, J. -L.; Bent, B. E. *J. Phys. Chem.* **1992**, *96*, 8529–8538.
- (37) Jenks, C. J.; Paul, A.; Smoliar, L. A.; Bent, B. E. *J. Phys. Chem.* **1994**, *98*, 572–578.
- (38) Andryushechkin, B. V.; Eltsov, K. N.; Shevlyuga, V. M. *Surf. Sci.* **2004**, *566-568*, 203–209.
- (39) Du, W. -L.; Xu, Y. -L.; Xu, Z. -R.; Fan, C. -L. *Nanotechnology* **2008**, *19*, 085707 (5pp).
- (40) Du, W. -L.; Niu, S. -S.; Xu, Y. -L.; Xu, Z. -R.; Fan, C. -L. *Carbohydr. Polym.* **2009**, *75*, 385–389.
- (41) Gottardi, W. Iodine and Iodine Compounds. In *Disinfection, Sterilization, and Preservation*, 4th ed.; Bloc, S.S., Ed.; Lea and Febiger: Philadelphia, PA, 1991; pp 152–166.
- (42) Gottardi, W. *Arch. Pharm. Med. Chem.* **1999**, *332*, 151–157.
- (43) Sudarshan, N. R.; Hoover, D. G.; Knorr, D. *Food Biotechnol.* **1992**, *6*, 257–272.
- (44) Helander, I. M.; Nurmiäho-Lassila, E. -L.; Ahvenainen, R.; Rhoades, J.; Roller, S. *Int. J. Food Microbiol.* **2001**, *71*, 235–244.
- (45) Rabea, E. I.; Badawy, M. E. -T.; Stevens, C. V.; Smaghe, G.; Steurbaut, W. *Biomacromolecules* **2003**, *4*, 1457–1465.
- (46) Sanpui, P.; Murugadoss, A.; Durgaprasad, P. V.; Ghosh, S. S.; Chattopadhyay, A. *Int. J. Food Microbiol.* **2008**, *124*, 142–146.
- (47) Li, J.; McLandsborough, L. A. *Int. J. Food Microbiol.* **2001**, *53*, 185–193.
- (48) Wilson, W. W.; Wade, M. M.; Holman, S. C.; Champlin, F. R. *J. Microbiol. Meth.* **2001**, *43*, 153–164.
- (49) Borkow, G.; Gabbay, J. *Curr. Med. Chem.* **2005**, *12*, 2163–275.